

Eddy current interactions in a Ferromagnet-Normal metal bilayer structure, and its impact on ferromagnetic resonance lineshapes

Vegard Flovik* and Erik Wahlström

Department of Physics, Norwegian University of Science and Technology, N-7491 Trondheim, Norway

Ferran Macià

Grup de Magnetisme, Dept. de Física Fonamental, Universitat de Barcelona, Spain

Andrew D. Kent

Department of Physics, New York University, 4 Washington Place, New York, New York 10003, USA

(Dated: May 14, 2022)

We investigate the effect of eddy currents on ferromagnetic resonance (FMR) in ferromagnet-normal metal (FM/NM) bilayer structures. Eddy currents are usually neglected for NM layer thicknesses below the microwave (MW) skin depth ($\simeq 800$ nm for Au at 10 GHz). However, we show that in much thinner NM layers (10-100 nm of Au or Cu) they induce a phase shift in the FMR excitation that results in a strong asymmetry of the measured absorption lines. In contrast to typical eddy-current effects, the asymmetry is larger for thinner NM layer and is tunable through changing the sample geometry and the NM layer thickness.

Eddy currents are induced currents in conductors by changing magnetic fields. These currents flow in closed loops perpendicular to the driving fields, and produce additional Oersted fields that partially compensate the external driving fields. Although eddy-current effects are usually neglected in metals with thicknesses below their electro-magnetic skin depth ($\simeq 800$ nm for bulk Au at 10 GHz), some studies have shown that the effects may be important for normal metal (NM) films far below the skin depth [1, 2]. In these studies it was predominantly the microwave-screening effects that were considered [3–5], and little attention was paid to how the induced Oersted fields can effect the magnetization dynamics in an adjacent ferromagnetic thin film.

Ferromagnetic resonance (FMR) spectroscopy experiments probe static and dynamic properties of magnetic materials. The technique relies on measuring the microwave absorption associated to the precession of the magnetization. In FMR experiments position and width of absorption lines carry valuable information about material parameters such as anisotropy fields and magnetic damping [6]. Further, recent experiments have used differences in symmetry of the FMR lines to study the spin pumping from a magnetic material to a normal metal [7–9]. Hence, to correctly interpret experimental data involving FMR it is important to understand how eddy currents—even in very thin films—can cause modifications in the measured FMR lineshape.

In this Letter we investigate the contribution of eddy currents to the FMR absorption lines in ferromagnet-normal metal (FM/NM) bilayer structures. We have systematically studied how the sample geometry and NM thickness affects the coupling between microwave (MW) fields and eddy-current-induced fields, and we show that

this coupling is tunable through changing the sample geometry and the NM layer thickness.

Experiments were performed with Permalloy (Py= $\text{Fe}_{20}\text{Ni}_{80}$) as the ferromagnet layers, and gold (Au) and Copper (Cu) as NM layers. The Py was grown by E-beam evaporation on oxidized silicon substrates, and the Au and Cu layers were grown by DC Magnetron sputter deposition. We controlled the thickness of the deposited NM layers using a Veeco Dektak 150 profilometer, and we cut our samples using a Dynatex DX-III combined scribe and breaker to obtain well defined sample geometries. Ferromagnetic resonance measurements were carried out in a commercial EPR setup (Bruker Bio-spin ELEXSYS 500).

The ferromagnetic resonance is usually driven directly by the MW field from a cavity or from a waveguide. However, capping a FM sample with a NM layer leads to circulating eddy currents in the NM, and additional Oersted fields in the FM. These Oersted fields have a different phase with respect to the MW fields—there is a phase lag between the MW fields and the induced currents—, and this results in a distortion of the FMR lineshape. A sketch of the FM/NM bilayer geometry and the path of the induced eddy currents flowing mainly along the sample edges [10, 11] is shown in Fig. 1a. Fig. 1b and c compares two representative FMR lineshapes for a 10 nm Py sample before and after capping it with 10 nm Au; although resonance frequency and width stay constant, the lineshape changes considerably.

To understand the origin of the distorted lineshapes due to the induced eddy currents, we consider a model describing the magnetization dynamics of the FM, starting from the Landau Lifshitz Gilbert equation:

$$\frac{\partial \mathbf{M}}{\partial t} = -\gamma \mathbf{M} \times \mathbf{H}_{\text{eff}} + \frac{\alpha}{M_s} \left(\mathbf{M} \times \frac{\partial \mathbf{M}}{\partial t} \right), \quad (1)$$

* vegard.flovik@ntnu.no

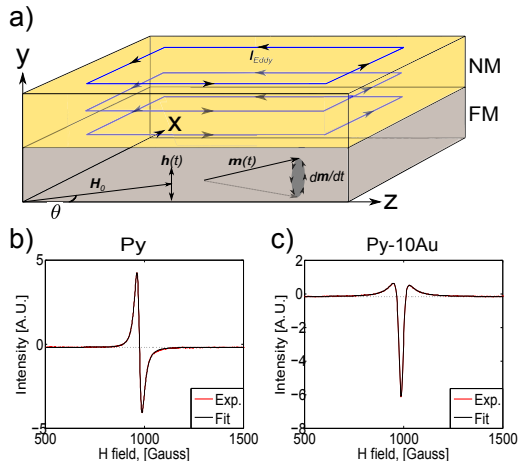


FIG. 1. (a) A schematic plot of the sample geometry showing the path of the induced eddy currents flowing mainly along the sample edges [10], [11]. (b) and (c) FMR lineshapes for a sample with 10 nm Py (b), and the same sample after being capped with 10 nm Au (c).

where γ is the gyromagnetic ratio, α is the Gilbert damping parameter, and M_s is the saturation magnetization. The effective magnetic field, \mathbf{H}_{eff} , includes the external field \mathbf{H}_0 and the anisotropy field, \mathbf{H}_A . We neglect the effects of dipole and exchange fields. A driving oscillatory field, \mathbf{h}_{ac} , composed of MW fields and fields induced by the eddy currents can be written as $\mathbf{h}_{\text{ac}}(t) = \mathbf{h}_{\text{MW}}e^{i\omega t} + \mathbf{h}_{\text{ind}}e^{i(\omega t + \phi)}$, where ϕ is the phase difference between the MW field and the induced field. The combined driving field can then be written in the form: $\mathbf{h}_{\text{ac}}(t) = \mathbf{h}e^{i\omega t}(1 + \beta i)$, where the parameter β accounts for the relative magnitude of the two fields and their phases.

We assume the external applied field, \mathbf{H}_0 , is along \mathbf{z} in the film plane (see Fig. 1a) and that the perturbations of the oscillatory field, \mathbf{h}_{ac} , are perpendicular to the external applied field (the components in the direction of the applied field do not directly perturb the dynamics of \mathbf{M}). The magnetization $\mathbf{M}(t)$ is then taken of the form $\mathbf{M}(t) = M_0\mathbf{z} + \mathbf{m}e^{i\omega t}$, where $\mathbf{m} \perp \mathbf{z}$. The magnetic response to small excitation fields, $\mathbf{m} = \chi\mathbf{h}$, is determined by the dynamic susceptibility tensor χ , with elements determined by solving Eq. 1. The observable quantity in FMR experiments is the MW power absorption, which is proportional to the imaginary part of the diagonal elements, $\Im(\chi_{xx})$. In our set-up the microwave frequency is fixed at 9.4 GHz, and the magnetic field H_0 is then swept to locate the Ferromagnetic resonance at the resonance field, $H_0 = H_R$, satisfying the condition $f_R = \gamma\sqrt{H_R(H_R + 4\pi M_s)}$. Taking this into account, and using the fact that the linewidth of the resonance is small compared to the resonance frequency, $\Im(\chi_{xx})$ can be rewritten up to an unimportant proportionality factor

as (See supplemental material):

$$\chi \propto \frac{1 + \beta(H_0 - H_R)/\Gamma}{(H_0 - H_R)^2 + (\Gamma/2)^2}, \quad (2)$$

where the parameter $\Gamma = 2\alpha\omega$ has been introduced to describe the linewidth. This expression consists of two components: a symmetric Lorentzian absorption line arising from the in-phase driving fields, and an antisymmetric line proportional to β arising from out-of-phase driving fields. The parameter β can thus be used as a direct measure of the phase shift effects due to eddy currents. Our FMR experiments were performed with a low amplitude ac modulation of the static field, which allows lock-in detection to be used in order to increase the signal to noise ratio. The measured FMR signal is then proportional to the field derivative of the imaginary part of the susceptibility. The experimental data was thus fitted to the derivative of Eq. 2, $\partial\chi/\partial H$ (i.e., we measure an absorption line as in Fig. 1b if the driving field has only the MW component; we measure an absorption line as in Fig. 1c if the driving field has a strong component from the eddy-current induced fields).

We first focus on the effect of the sample geometry. A full in-plane 360 degrees rotation of a sample of dimensions 1×3 mm with a thickness of 10 nm Py capped with 10 nm Au is shown in Fig. 2a, where $\theta = 0$ corresponds to an applied field, H_0 , parallel to the short side of the sample. We note that although the asymmetry, β , has varied considerably, the resonance field H_R was not effected by the sample rotation (neither was it by the capping with Au or Cu).

To investigate the effect of sample geometry further, a set of samples of dimensions $1 \times L$ mm, where L ranged from 0.5 to 4 mm was studied. The samples were again of 10 nm Py capped with 10 nm Cu and 5 nm Ta to prevent oxidation. We notice that the sample length in the direction parallel to the applied field, H_0 , is the main parameter that determines the asymmetry of the FMR lineshapes, given by the parameter β . Fig. 2b shows the dependence of sample length when the varying dimension is parallel to the applied field, H_0 . We see that the asymmetry increases with the sample's length and reaches a value where β appears to diverge at a length of about 3.3 mm. Samples with a length below 1 mm have lineshapes almost identical to samples with no NM capping.

We consider now the basic physics to describe the above results. The induced eddy currents flow in closed loops in planes perpendicular to the MW magnetic field, which is perpendicular to the film plane in our experiment. Thus, to obtain circulating eddy currents as shown in Fig. 1a depends on having the MW field perpendicular to the film plane. We have conducted control experiments where the MW fields were applied in the film plane and we observed that the FMR lineshapes were always symmetric, indicating there were no observable effect of the eddy currents.

In our experimental geometry (see Fig. 1a), the in-

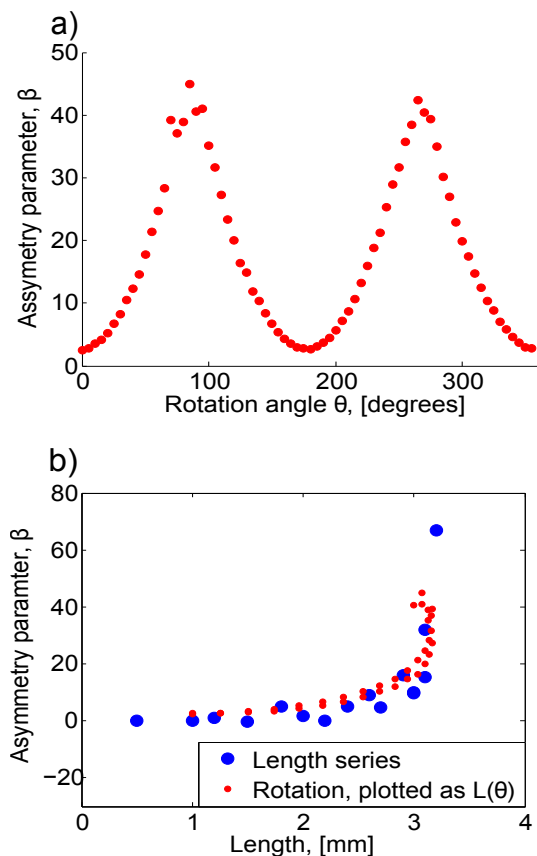


FIG. 2. (a) Angular dependence of the β parameter describing the FMR lineshape for a sample of 10 nm Py capped with 10 nm Au with dimensions 1×3 mm; the applied field is rotated 360 degrees in the film plane. (b) Sample length dependence of β for samples of 10 nm Py capped with 10 nm Cu (and 5 nm Ta to prevent oxidation) of dimension $1 \times L$ mm, i.e. each datapoint in the "Length series" corresponds to a separate sample of length L . We also plotted in (b) the rotational measurements shown in (a) for a single sample, considering that the effective length in the direction of the applied field, H_0 , is approximated by $L(\theta) = l \sin(\theta) + w \cos(\theta)$, $l = 3$ mm and $w = 1$ mm.

duced eddy currents flow mainly in circulating paths along the sample edges [10], [11]. The induced Oe fields have a component in the film plane and another perpendicular to the film plane. For the sample edges that are parallel to the applied field, H_0 , the Oersted fields will have the main in-plane component perpendicular to the applied field, H_0 , and could thus affect the FMR of the Py film. On the other hand, currents along sample edges perpendicular to the applied field, H_0 , will give rise to an in-plane Oersted field that is parallel to the applied field, H_0 , and should not affect the FMR response. The observed strong rotational dependence (See, Fig. 2b), suggest that the effective driving field has an important contribution in the sample plane; the contribution from the component perpendicular to the sample plane should not depend on the direction of the sample edges with respect to the applied field, H_0 .

The asymptotic behavior of β as the sample length in-

creases can be understood by considering how the sample size effects the magnitude of the induced currents. We estimate the current path as a rectangular loop of length l , width w , and cross section σ . The induced electromotive force (EMF) is then given by the rate of change of magnetic flux through the area enclosed by the loop; its absolute value is given by $|\epsilon| = lw \left| \frac{\partial h}{\partial t} \right| \propto lw h_{MW} 2\pi f$, where f and h_{MW} are the MW frequency and amplitude respectively. The resistance of such a loop is given by $R = 2\rho(l+w)/\sigma$, where ρ is the resistivity of the NM and σ the cross section of the current path. The induced current is finally given by $I = \epsilon/R$. We consider as an approximation that the magnetic field resulting from a current I in such a plane is given by $h_{ind} = \mu_0 I / 2\zeta$, where ζ is the width of the current path and μ_0 is the vacuum permeability. The expression for the induced field is thus proportional to the sample size. We calculated the induced field for a square sample, $w = l$, of 10 nm thickness. Using the resistivity data for thin metal films from [2], and in the presence of a MW field of 9.4 GHz and $6 \mu\text{T}$, we obtained that at a dimension of about 2×2 mm the induced field equals the MW field. Our estimated value corresponds well with what we see in the experiments: when the sample size approaches the mm scale the effects become increasingly important.

We compare now the length series with the rotational measurements by using a simple geometric approximation: we consider that the length of the sample parallel to the applied field, H_0 is given by $L(\theta) = l \sin(\theta) + w \cos(\theta)$, where l and w are the length (3 mm) and width (1 mm) of the sample, and $\theta = 0$ corresponds to the applied field parallel to the short side of the sample. We have plotted in Fig. 2b the rotational measurements following this approach and we can see that the resulting curve is almost identical to the length series.

We designed a control experiment that consisted in taking a large sample of dimensions 1×3 mm and dividing it into electrically isolated regions of 1×1 mm with an automated scriber that scratched the sample without breaking it—we limited the size of the possible current loops. We tested this in samples with no capping and the FMR signal was not effected. However, the same procedure on a sample capped with 10 nm Au presented a remarkable effect: the lineshape before scratching the sample was strongly asymmetric, but after scratching the film it returned to being symmetric again and matched the lineshapes for a sample of dimensions 1×1 mm.

Next, we focus on another important parameter that governs the effect of eddy currents: the thickness of the NM layer. We prepared samples with a NM (both with Au and Cu) thickness ranging from 10 to 100 nm. The experiments presented here were also performed in two more samples, where we obtained the same results. The measured asymmetry parameter β as a function of NM thickness is shown in fig. 3 for a sample of dimensions 1×3 mm, with the applied field parallel to the long side of the sample. Replacing the Au layer by Cu shows a similar

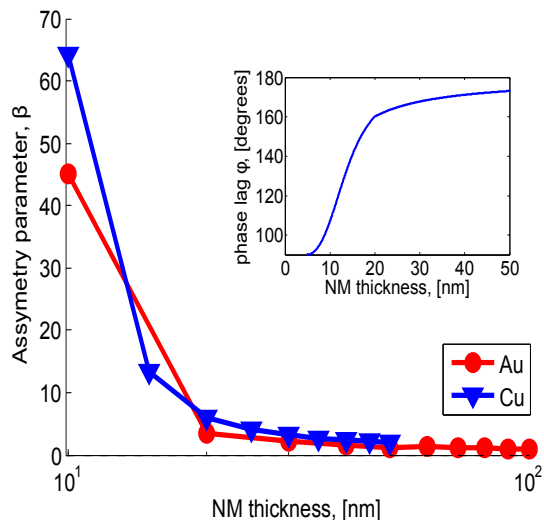


FIG. 3. NM thickness dependence of the β parameter describing the FMR lineshape for a sample of dimension 1×3 mm with the applied field, H_0 , parallel to the long side of the sample. Comparing Au and Cu as NM layer in the region 0-50nm. Inset: Thickness dependence of the phase shift, ϕ , between the MW field and induced field.

behavior; the thicker the NM, the more symmetric the FMR lineshapes.

To explain the thickness dependence we use a simplified model where we assume that induced eddy currents circulate in two dimensional planes in the NM layer. The Oersted fields originated by the eddy currents have a phase, ϕ , compared to the external MW field, which in the ideal case of no inductance is expected to be $\phi = \pi/2$. However, due to the inductance of the NM film, there will be an additional phase between the MW field and the induced field that depends strongly on the NM thickness. We can write the phase as $\phi = \pi/2 + \tan^{-1}(\frac{\omega L}{R})$, where ω is the microwave frequency, L and R are the inductance and resistance of the film.

We take an approximate value for the inductance $L \approx 10^{-8}$ H [12] considering a rectangular current path along the edges of the NM layer, and sample dimensions of $w=1$ mm and $l=3$ mm. We estimate the film resistance, R , as a function of the thickness by introducing a correction factor, η , that describes the correction to the film conductivity compared to the bulk value for a thickness below the electron mean free path [2].

We have computed the phase shift between the MW field and the induced field accounting for the sample size

and material parameters (we considered η to be a linear function of the film thickness compared to the mean free path, l_{mfp} : $\eta = \min(1, \frac{\delta}{l_{\text{mfp}}})$, where δ is the NM thickness. The inset of Fig. 3 shows the thickness dependence of the phase shift, ϕ ; at thick NM the phase difference approaches an asymptotic value of π , which corresponds to $\beta = 0$ (i.e., the asymmetric lineshapes disappear quickly as the NM thickness increases). This calculations agree well with the experimental data, where the asymmetry drops off quickly with the thickness.

We investigated thinner NM layers of 5 nm and the FMR lineshapes were similar to single Py films. We believe this is because we had non-continuous metal films for these thicknesses; Au films tend to be granular and the Cu films might have oxidized. We also investigated the thick film limit, and deposited NM layers of 150, 200, 500, 750 and 1000 nm Au. For a thickness above approx 500 nm, the lineshapes appeared slightly asymmetric again. However, the model we have used to investigate the effects of eddy currents assumes that the current flows in two dimensional planes in the NM and this is no longer valid for these thicknesses.

To summarize, we have shown that induced eddy currents can play an important role in FM/NM bilayer structures for certain sample geometries. The dynamics of the system is determined by the interplay of the MW fields and induced fields by eddy currents, and we have shown that this coupling is tunable through changing the sample geometry and the NM layer thickness. The tunability of the coupling opens up possibilities to use patterned NM structures to tailor the local field geometry and phase of the induced microwave fields, which could be of importance for spintronics applications.

ACKNOWLEDGEMENTS

We are grateful for insightful discussions with A. Brataas and H. Skarsvåg. This work was supported by the Norwegian Research Council (NFR), project number 216700. V.F acknowledge partial funding obtained from the Norwegian PhD Network on Nanotechnology for Microsystems, which is sponsored by the Research Council of Norway, Division for Science, under contract no. 221860/F40. FM acknowledges support from Catalan Government through COFUND-FP7 and support from MAT2011-23698. A. D. K acknowledges support through the US-National Science Foundation, NSF-DMR-1309202.

-
- [1] S. Fahy, C. Kittel, S. G. Louie, American Journal of Physics 56, 989 (1988);
 [2] I. V. Antonets, L. N. Kotov, S. V. Nekipelov, and E. N. Karpushov, Technical Physics November 2004, Volume

- 49, Issue 11, pp 1496-1500
 [3] M. Bailleul, Appl. Phys. Lett. 103, 192405 (2013)
 [4] M. Kostylev J. Appl. Phys. 106, 043903 (2009)

- [5] I. S. Maksymov and M. Kostylev J. Appl Phys. 116, 173905 (2014)
- [6] M. Harder, Z. X. Cao, Y. S. Gui, X. L. Fan, and C.-M. Hu, Phys. Rev. B 84, 054423 (2011)
- [7] O. Mosendz, V. Vlaminck, J. E. Pearson, F. Y. Fradin, G. E. W. Bauer, S. D. Bader, and A. Hoffmann, Phys. Rev. B 82, 214403 (2010)
- [8] O. Mosendz, J. E. Pearson, F. Y. Fradin, G. E. W. Bauer, S. D. Bader, and A. Hoffmann, Phys. Rev. Lett. 104, 046601 (2010)
- [9] L. Liu, T. Moriyama, D. C. Ralph, and R. A. Buhrman, Phys. Rev. Lett. 106, 036601 (2011)
- [10] M. Krakowski Archiv für Elektrotechnik 64 (1982) 307-311
- [11] G. De Mey, Archiv für Elektrotechnik 1974, Volume 56, Issue 3, pp 137-140
- [12] F. W. Grover Inductance Calculations 2004

I. SUPPLEMENTAL MATERIAL

A. Susceptibility tensor elements

We consider a model describing the magnetization dynamics of the FM starting from the Landau Lifshitz Gilbert equation, as defined in the main text.

$$\frac{\partial \mathbf{M}}{\partial t} = -\gamma \mathbf{M} \times \mathbf{H}_{\text{eff}} + \frac{\alpha}{M_s} \left(\mathbf{M} \times \frac{\partial \mathbf{M}}{\partial t} \right). \quad (3)$$

The elements of χ was determined by solving eq(1), and discarding higher order terms. Setting $\vec{m} = \chi \vec{h}$ and introducing $\omega_0 = \gamma H$ and $\omega_M = \gamma M_0$, this gives:

$$\chi = \begin{pmatrix} \chi_{xx} & i\chi_{xy} \\ -i\chi_{yx} & \chi_{yy} \end{pmatrix} \quad (4)$$

Where the matrix elements are given by

$$\chi_{xx} = \chi_{yy} = \frac{(1 + \beta i)\omega_M(\omega_0 + i\alpha\omega)}{\omega_0^2 - \omega^2(1 + \alpha^2) + 2i\alpha\omega\omega_0} \quad (5)$$

$$\chi_{xy} = \chi_{yx} = \frac{(1 + \beta i)\omega\omega_M}{\omega_0^2 - \omega^2(1 + \alpha^2) + 2i\alpha\omega\omega_0} \quad (6)$$

One can then separate the real and imaginary part of the diagonal elements χ_{xx} and χ_{yy} . Assuming low damping ($\alpha^2 \approx 0$), this gives the following:

$$\Re(\chi_{xx}) = \frac{\omega_0\omega_M(\omega_0^2 - \omega^2) + \beta\alpha\omega\omega_M(\omega_0^2 + \omega^2)}{(\omega_0^2 - \omega^2)^2 + (2\alpha\omega\omega_0)^2} \quad (7)$$

$$\Im(\chi_{xx}) = \frac{-\alpha\omega\omega_M(\omega_0^2 + \omega^2) + \beta\omega_0\omega_M(\omega_0^2 - \omega^2)}{(\omega_0^2 - \omega^2)^2 + (2\alpha\omega\omega_0)^2} \quad (8)$$

As the FMR linewidth for permalloy films is small compared to the resonance frequency, one can assume that one does not need to deviate far from the resonance in order to observe the shape of the curve. That being the case, $\omega_0^2 + \omega^2 \approx 2\omega_0^2$, and

$$(\omega_0^2 - \omega^2)^2 = (\omega_0 + \omega)^2(\omega_0 - \omega)^2 \approx 4\omega_0^2(\omega_0 - \omega)^2 \quad (9)$$

Hence, for narrow linewidths, eq.(8) is well approximated by:

$$\Im(\chi_{xx}) \approx \left(\frac{\omega_M\Gamma}{4} \right) \frac{-1 + \beta(\omega_0 - \omega)/\Gamma}{(\omega_0 - \omega)^2 + (\Gamma/2)^2} \quad (10)$$

Where the parameter $\Gamma = 2\alpha\omega$ has been introduced to describe the linewidth. In our FMR experiments the microwave frequency is fixed at 9.4GHz, and the external magnetic field H is then swept to locate the Ferromagnetic resonance at the resonance field $H = H_R$. To extract the parameter β from our experiments we rewrite eq.(10), and neglect an unimportant proportionality factor:

$$\chi \propto \frac{1 + \beta(H_0 - H_R)/\Gamma}{(H_0 - H_R)^2 + (\Gamma/2)^2} \quad (11)$$

B. Self inductance of current loop

Approximating the current path in the NM layer as a rectangular loop consisting of a wire with length l , width w and cross section σ , the inductance is given by [12]:

$$L = \frac{\mu_0\mu_r}{\pi} \left[-2(w+l) + 2\sqrt{l^2 + w^2} - l * \ln \left(\frac{l + \sqrt{l^2 + w^2}}{w} \right) \right] \quad (12)$$

$$-w * \ln \left(\frac{w + \sqrt{l^2 + w^2}}{l} \right) + l * \ln \left(\frac{2l}{\sigma} \right) + w * \ln \left(\frac{2w}{\sigma} \right) \quad (13)$$